This is a preprint, the final version is subject to change, of the American Mineralogist (MSA)
Cite as Authors (Year) Title. American Mineralogist, in press.
(DOI will not work until issue is live.) DOI: http://dx.doi.org/10.2138/am-2017-5856

Revision 1

Title: Effect of composition on compressibility of skiagite-Fe-majorite garnet

Authors: Leyla Ismailova[1,2,3], Maxim Bykov[1], Elena Bykova[1], Andrei Bobrov[4], Ilya Kupenko[1,5,6], Valerio Cerantola[1,5], Denis Vasiukov[1,2], Natalia Dubrovinskaia[2], Catherine McCammon[1], Michael Hanfland[5], Konstantin Glazyrin[7], Hanns-Peter Liermann[7], Alexander Chumakov[5], Leonid Dubrovinsky[1]

Affiliations:

[1]Bayerisches Geoinstitut, University of Bayreuth, Universitätsstraße 30, D-95440 Bayreuth, Germany.

[2]Laboratory of Crystallography, University of Bayreuth, Universitätsstraße 30, D-95440 Bayreuth, Germany

[3] Vernadsky Institute of Geochemistry and Analytical Chemistry, Russian Academy of Sciences, 19 ul. Kosygina, Moscow 119991, Russia

[4]Department of Petrology, Geological Faculty, Moscow State University, 119991 Moscow, Russia

[5]ESRF-The European Synchrotron CS40220 38043 Grenoble Cedex 9 France

[6]Institut für Mineralogie, University of Münster, Corrensstr. 24, 48149 Münster, Germany

[7]Photon Sciences, Deutsches Elektronen-Synchrotron, Notkestrasse 85, D-22603 Hamburg, Germany.

*Correspondence to: leyla.isml@gmail.com

Abstract

Skiagite-Fe-majorite garnets were synthesized using a multianvil apparatus at 7.5-9.5 GPa and 1400-1600 K. Single-crystal X-ray diffraction at ambient conditions revealed that synthesized garnets contain 23 to 76 % of an Fe-majorite component. We found that the substitution of Fe^{2+} and Si^{4+} for Fe^{3+} in the octahedral site decreases the unit-cell volume of garnet at ambient conditions. Analysis of single-crystal X-ray diffraction data collected on compression up to 90 GPa of garnets with different compositions reveals that with increasing majorite component the bulk modulus increases from 159(1) to 172(1) GPa. Our results and literature data unambiguously demonstrate that the total iron content and the Fe^{3+}/Fe^{2+} ratio in (Mg,Fe)-majorites have a large influence on their elasticity. At pressures between 50 and 60 GPa we

observed a significant deviation from a monotonic dependence of the molar volumes of skiagite-Fe-majorite garnet with pressure, and over a small pressure interval the volume dropped by about 3%. By combining results from single-crystal X-ray diffraction and high-pressure synchrotron Mössbauer source spectroscopy we demonstrate that these changes in the compressional behavior are associated with changes of the electronic state of Fe in the octahedral site.

Keywords: skiagite-majorite garnet; single-crystal X-ray diffraction; Mössbauer spectroscopy; equation of state; upper-mantle; transition zone

1. Introduction

Garnets are among the most abundant phases in the upper mantle and transition zone; hence data on their behavior under extreme conditions is important for understanding the composition, structure, and dynamics of the deep Earth's interior. According to the pyrolite composition model, the Earth's upper mantle below 50 km is dominated by four major phases: olivine ($(Mg,Fe)_2SiO_4$), orthopyroxene ($(Mg,Fe)SiO_3$), clinopyroxene ($(Ca(Mg,Fe^{2+})Si_2O_6$), and garnet ($(Mg,Fe,Ca)_3(Al,Fe,Cr)_2Si_3O_{12}$) (Ringwood 1975; Ita and Stixrude 1992). With increasing pressure, upper mantle minerals undergo several important phase transitions. Olivine transforms to wadsleyite at a pressure of ~13.5 GPa, and then to ringwoodite at ~18 GPa (Irifune et al. 2008). Ortho- and clinopyroxene progressively dissolve in garnet, resulting in an excess of Mg and Si in the structure. The volume fraction of garnet thereby increases from ~10 % to ~40% or more in the transition zone, where garnet(s) become majoritic (Si-rich) (Duffy and Anderson 1989; Irifune et al. 2008; Wood et al. 2013).

Natural garnets are usually complex solid solutions because the garnet structure can accommodate a number of different divalent and trivalent cations. High-pressure garnet endmembers include Mg-majorite $Mg_4Si_4O_{12}$, Fe^{2+}-majorite $Fe^{2+}{}_4Si_4O_{12}$, Na-majorite

57 $Na_2MgSi_5O_{12}$ (Bobrov et al. 2008) and knorringite $Mg_3Cr_2Si_3O_{12}$ (Bykova et al., 2013;
58 Dymshits et al., 2014). While most cations in garnet occur in a single oxidation state (Al^{3+},
59 Ca^{2+}, Mg^{2+}, Cr^{3+}), iron commonly occurs as both Fe^{2+} and Fe^{3+}. The major Fe^{3+}-bearing
60 garnets are andradite ($Ca_3Fe_2Si_3O_{12}$), khoharite ($Mg_3Fe_2Si_3O_{12}$), and skiagite ($Fe_3Fe_2Si_3O_{12}$)
61 (Amthauer et al., 1976; Luth et al., 1990; Woodland and Ross, 1994; Ismailova et al., 2015).
62 Skiagite garnet is important for the description of phase equilibria in mantle rocks. At
63 a fixed oxygen fugacity relative to a standard buffer such as fayalite-magnetite-quartz (FMQ),
64 garnet will be increasingly enriched in Fe^{3+} with increasing pressure (Wood et al. 1996).
65 Similarly, with increasing depth, garnet with fixed ferric iron content will be stabilized at
66 progressively lower oxygen fugacity relative to the FMQ buffer.(Wood et al. 2013). With
67 increasing pressure $Fe^{3+}/\sum Fe$ may also increase due to the redistribution of Fe^{3+} from
68 clinopyroxene to garnet (Woodland and Koch 2003) due to the expanding skiagite stability
69 field. At greater depths, skiagitic garnet accommodates an excess of Si that stabilizes a solid
70 solution with Fe^{2+}-majorite ($Fe_4Si_4O_{12}$) (Woodland et al., 2009; Ismailova et al., 2015).
71 Mössbauer spectroscopy studies on garnet indicate that Fe^{3+} occupies an octahedral
72 site (e.g., Amthauer et al., 1976). Thus, it is important to study the effect(s) of the majoritic
73 substitution ($2Fe^{3+} \leftrightarrow Fe^{2+}+Si^{4+}$) in the octahedral position. There is additional interest in
74 studies of iron in garnets at high pressure due to the possibility of compression-induced spin-
75 crossover (Friedrich et al. 2014, 2015; Stan et al. 2015).
76 In this paper we report the results of a study of synthetic pure-iron skiagite-majorite
77 garnet with different compositions using single crystal X-ray diffraction and synchrotron
78 Mössbauer source spectroscopy up to 90 GPa. We combine our data with those reported
79 earlier for different garnets in order to evaluate the effect of majoritic substitution on material
80 properties.
81

82 **2. Methods**

Iron-bearing skiagite-majorite garnets with different compositions were synthesized from stoichiometric mixtures of pure oxides: SiO_2, Fe_2O_3, and $Fe_{1-x}O$. For Mössbauer spectroscopy experiments starting material was enriched with ^{57}Fe. High temperatures and high pressures were generated using a Kawai-type multi-anvil apparatus at Bayerisches Geoinstitut (Bayreuth, Germany). Experimental conditions and compositions are listed in Table 1. More details of the synthesis experiments can be found in Ismailova et al., (2015).

Crystals for single-crystal X-ray diffraction studies were selected based on the quality of their diffraction peak profiles using an *in-house* high-brilliance rotating anode diffractometer at Bayerisches Geoinstitut (Bayreuth, Germany). Pre-selected isometric crystals of ~10 μm in the longest dimension were loaded in diamond anvil cells (DACs) into holes drilled through Re gaskets indented to 20-35 μm thickness. First, the single-crystal data were collected at ambient conditions. After that DACs were loaded with Ne at ~1.4 kbar. Neon serves as a quasi-hydrostatic pressure transmitting medium. Below 10 GPa the pressure was determined from ruby fluorescence, while above 10 GPa we used the diffraction lines of crystallized Ne to determine the pressure (Fei et al. 2007). We used Boehler-Almax diamond anvils with 250 μm culets for measurements up to ~60 GPa, and beveled diamonds with 120 μm culets were used to achieve pressures up to 90 GPa.

Garnets with composition $Ski_{69}Maj_{31}$, $Ski_{54}Maj_{46}$, $Ski_{24}Maj_{76}$ were loaded into the same DAC at a distance of ~10-15 μm from each other. In order to achieve a perfect alignment of the cell, a small particle of W was loaded along with three single crystals and a ruby chip. First, the W particle was aligned in the beam, using it's strong absorption. Secondly, garnet single crystals were aligned using the optical camera, using the position of the W particle as a reference.

Single-crystal X-ray diffraction experiments were performed at the beamline ID09A at ESRF, Grenoble, France (λ= 0.4151 Å; beam size, 10 × 10 μm^2) (Merlini and Hanfland, 2013) and at the extreme conditions beamline ECB P02.2 at PETRA III, DESY, Hamburg,

Germany (λ= 0.2903 Å; beam size, 3 × 8 μm^2) (Liermann et al. 2015). Diffraction images were collected at various pressures using the following strategy: wide scans were collected during ω rotation scans of ±20° with 40 seconds per frame; step scans were collected with rotation of the cell of ±38° with a typical exposure time 0.5-1 seconds per frame. The indexing of Bragg reflections, the intensity data reduction and the empirical absorption correction were performed with the Agilent™ CrysAlisPro software (Oxford Diffraction 2006). Crystal structures were refined using Jana2006 (Petříček et al. 2014). Polyhedral volumes were calculated using VESTA software (Momma and Izumi 2011). The Birch-Murnaghan and Vinet equations of state coefficients were refined using the program EoSFit-7c (Angel et al. 2014).

Synchrotron Mossbauer Source (SMS) spectra were recorded at the Nuclear Resonance Beamline ID18 at ESRF using the (111) Bragg reflection of a $^{57}FeBO_3$ single crystal mounted on a Wissel velocity transducer driven with a sinusoidal wave form (Rüffer and Chumakov 1996). The X-ray beam was focused to 20 μm vertical and 10 μm horizontal dimensions using Kirkpatrick-Baez mirrors. The linewidth of the SMS and the absolute position of the center shift (CS) were controlled before and after each measurement using a $K_2Mg^{57}Fe(CN)_6$ reference single line absorber. The velocity scale was calibrated using a 25 μm thick natural α-Fe foil. Each spectrum took ~ 1-24 hours to collect. Spectra were fitted using a full transmission integral with a normalized Lorentzian-squared source line shape using the MossA software package (Prescher et al. 2012).

3. Results/results and discussion

3.1 Structures of skiagite-Fe-majorite garnets at ambient conditions

Single crystals of garnets were measured first at ambient conditions. Synthesis conditions, compositions, unit-cell volumes, and crystallographic data of skiagite-majorite garnets collected at ambient conditions are given in **Table 1.** All garnets have structures with a cubic

space group $Ia\bar{3}d$ (#230) symmetry. The structural refinement revealed that the dodecahedral and tetrahedral sites are fully occupied by Fe and Si atoms, respectively. The octahedral site is also fully filled, but has a mixed (Fe and Si) occupancy.

Structural refinement also revealed that the synthesized garnets contain from 23.4(1) mol. % to 76(5) mol. % of the end member iron-majorite ($Fe_4Si_4O_{12}$). An increase in Fe-majorite content causes a decrease in the molar volume of the garnet (**Fig. 1**)**.** If we linearly extrapolate our data along the iron majorite-skiagite join, we obtain a unit cell volume for pure majorite $Fe_4Si_4O_{12}$ of 1589.2 $Å^3$, which is higher than the value obtained by Akaogi and Akimoto (1977) (1558.89 $Å^3$) from extrapolation of iron majorite ($Fe_4Si_4O_{12}$)-almandine ($Fe_3Al_2Si_3O_{12}$) solubility data.

The crystal structure refinement shows that a change in the unit-cell volume is associated with a decrease in the (Fe,Si)-O bond length of $(Fe,Si)O_6$ octahedra. Variations in the bond length and polyhedral volumes are shown in **Table 2** in comparison with the values for pure skiagite predicted by Novak and Gibbs (1971). With increasing iron-majorite component along the skiagite-majorite join from (Ski_{100}) to (Ski_{24}), the bond length decreases from 1.98 Å to 1.957(5) Å, and the polyhedral volume reduces from 10.40 $Å^3$ (Ski_{100}) to 9.9780 $Å^3$ (Ski_{24}). Remarkably, garnet maintains cubic symmetry up to 76% of iron-majorite content. In pyrope-majorite garnets a transition from cubic to tetragonal symmetry occurs at 80 % of $Mg_4Si_4O_{12}$ (Heinemann et al. 1997); Na-majorite-pyrope remains cubic with up to 70% of Na-majorite component, and knorringite-majorite garnet - with up to 97% of Mg-majorite (Sirotkina et al. 2015)

3.2 Equation of state of skiagite-majorite garnets at pressures up to 50 GPa

For measurements at high pressure we used garnet single crystals with four different compositions along the skiagite-majorite join:

- **$Ski_{76.6}Maj_{23.4}$** $Fe^{2+}{}_3(Fe^{2+}{}_{0.234(2)}Fe^{3+}{}_{1.532(1)}Si^{4+}{}_{0.234(2)})Si_3O_{12}$;

- **$Ski_{69}Maj_{31}$** $Fe^{2+}_3(Fe^{2+}_{0.31(2)}Fe^{3+}_{1.39(2)}Si^{4+}_{0.31(2)})Si_3O_{12}$;

- **$Ski_{54}Maj_{46}$** $Fe^{2+}_3(Fe^{2+}_{0.46(2)}Fe^{3+}_{1.08(2)}Si^{4+}_{0.46(2)})Si_3O_{12}$;

- **$Ski_{24}Maj_{76}$** $Fe^{2+}_3(Fe^{2+}_{0.76(5)}Fe^{3+}_{0.48(5)}Si^{4+}_{0.76(5)})Si_3O_{12}$.

The unit cell volume variations with pressure were measured for $Ski_{76.6}Maj_{23.4}$ up to 89 GPa and for $Ski_{69}Maj_{31}$, $Ski_{54}Maj_{46}$, and $Ski_{24}Maj_{76}$ up to 60 GPa **(Fig. 2, Table S1-S4).** All studied garnets in the skiagite-majorite join show similar compressional behavior with unit cell volumes decreasing monotonically with pressure increase up to 50 GPa.

A drastic change in the compressional behavior appears at pressures above 50 GPa **(Fig. 2).** The pressure-volume relation obtained for $Ski_{76.6}Maj_{23.4}$ up to 89 GPa can be fit by two curves showing a clear discontinuity in the volume change at pressures between 50 and 60 GPa and a similar tendency is observed for other garnets (**Fig. 2**). In all cases the volume reduction in the interval of 40 to 50 GPa is about 3.1-3.5 %, while between 50 and 60 GPa it is about 4.7-5.5 %. Despite the clear discontinuity in the compressional behavior, no structural transitions were detected from the structure refinements and skiagite-majorite garnets maintained cubic symmetry even at highest pressures achieved. We refined the garnet structure at every pressure point and no changes were observed.

We used the pressure-volume (P-V) data up to 50 GPa and a 3rd order Birch-Murnaghan equation of state (EOS) to obtain the EOS parameters for the four investigated garnets **(Table 3).** The ambient pressure bulk moduli $K_{300,0}$ obtained in our study (164(3)-169(3) GPa) are systematically higher than that of pure skiagite $Fe_3Fe_2Si_3O_{12}$ (157.4(3.0) GPa, K´=6.7(8)) obtained by Woodland et al. (1999). The pressure derivatives of the bulk moduli (K´) in our fits are within the range 3.88(15) and 4.6(1).

3.3 Behavior of coordination polyhedra upon compression.

Accurate crystal structure refinement allows us to calculate the volumes of different polyhedra and follow them as a function of pressure. The skiagite-Fe-majorite solid solution

is characterized by the substitution of Fe^{3+} for Fe^{2+} and Si^{4+} in the octahedral site: $2Fe^{3+} \leftrightarrow Fe^{2+}+Si^{4+}$; the dodecahedral site is occupied exclusively by Fe^{2+} and the tetrahedral site is occupied only by Si^{4+} only. In order to avoid uncertainties introduced by correlations between K and K´ we fit the data using a 2nd order Birch-Murnaghan equation of state (K´=4). Results of the P-V fit (V_0 and $K_{300,0}$) for each individual polyhedron of studied garnets are given in **Table S5** *(Supplementary)* and the pressure dependence of the volumes for tetrahedra, octahedra, and dodecahedra for garnet with composition $Ski_{76.6}Maj_{23.4}$ are shown in **Fig. 3.**

As expected, SiO_4 tetrahedra are stiff with bulk moduli between 386 and 483 GPa. These values are typical for SiO_4 tetrahedra in silicate garnets and are in good agreement with data (327 to 434 GPa) reported earlier from both experimental and theoretical studies on silicate garnets (Milman et al. 2001; Friedrich et al. 2014, 2015). The $Fe^{2+}O_8$ polyhedra are much more compressible with bulk moduli of 101-115 GPa. At pressures up to about 50 GPa, the compressibility of $(Fe,Si)O_6$ octahedra for all studied garnets are similar and fall in the range 216-233 GPa. At 50 GPa iron-bearing octahedra show a drastic decrease in volume with a reduction of about 7 %**.** In contrast, FeO_8 and SiO_4 polyhedra show monotonically varying behavior upon compression up to the highest pressure achieved in this study **(Fig.3).**

3.4 Synchrotron Mössbauer source spectroscopy

Synchrotron Mössbauer source spectra of $Ski_{76.6}Maj_{23.4}$ garnet were collected at several pressures between ambient and 90 GPa (selected spectra are shown in **Fig. 4** and hyperfine parameters are presented in **Table 4**). Here we present the results directly related to the changes in garnet crystal structure observed above 50 GPa, while detailed spectral analysis and their interpretation will be published elsewhere. At pressures below ~50 GPa Mössbauer spectra contain two components – one with higher and one with lower center shift (CS) and quadrupole splitting (QS). The former has hyperfine parameters characteristic for Fe^{2+} in a dodecahedral oxygen environment while the latter may be assigned to mixed Fe^{2+} and Fe^{3+} in octahedra (**Fig. 4**). Up to 50 GPa, there are no any drastic changes in SMS spectra and

hyperfine parameters vary monotonically with pressure. Between 50 and 60 GPa there are notable changes in the appearance of the component corresponding to Fe^{3+}-dominated octahedra, while the component corresponding to Fe^{2+} in FeO_8 dodecahedra remains almost the same. There are several possibilities to fit spectra above 50 GPa. One is shown in **Fig. 4 (c)** with two components corresponding to $(Fe,Si)O_6$ octahedra – a doublet with CS even lower that those observed below 50 GPa but with higher QS, and a singlet with relatively high CS. Since CS of Fe^{3+} decreases and QS increases at the high spin to low spin crossover (Bengtson et al. 2009; Hsu et al. 2011), while low spin Fe^{2+} in octahedral environment is represented by a singlet (Kantor et al. 2006; Cerantola et al. 2015) we attribute the singlet and the doublet components to low spin Fe^{2+} and Fe^{3+}, respectively.

4. Discussion

4.1 Effect of spin transition on the compressibility

Recent experimental and theoretical studies on the iron spin and valence states in iron-bearing minerals suggest that pressure can induce spin-pairing transitions of Fe^{2+} and Fe^{3+} in relatively small octahedral sites such as in hematite Fe_2O_3 (Badro et al., 2002; Bykova et al., 2013), α-FeOOH (Xu et al. 2013), siderite $FeCO_3$ (Lavina et al. 2009; Cerantola et al. 2015), $CaFe_2O_4$ (Merlini et al. 2010), and $Y_3Fe_5O_{12}$ (Stan et al. 2015). The reported spin-pairing transitions occur over a broad pressure range of 40 to 60 GPa. For silicate garnets, the spin-transition of Fe^{3+} was previously observed only in andradite $Ca_3Fe_2Si_3O_{12}$ (Friedrich et al., 2014) in the pressure range of 60-70 GPa. Recently Friedrich et al. (2015) showed that Mn^{3+} can also undergo a spin transition, namely in silicate hydrogarnet henritermierite $Ca_3Mn_2[SiO_4]_2[O_4H_4]$, but the spin transition starts at a slightly lower pressure (55-70 GPa).

As seen in our X-ray diffraction and Mössbauer spectroscopy data for skiagite-Fe-majorite garnet, there are changes in both octahedral Fe^{3+} and Fe^{2+} between 50 and 60 GPa.

The transformation is associated with a notable volume collapse that we assign to spin-paring. To obtain the EOS coefficients of skiagite-majorite garnet $Ski_{76.6}Maj_{23.4}$ below and above the spin crossover, we used the P-V X-ray diffraction data in two pressure intervals. The spin transition causes a reduction of the garnet unit cell volume by ~3%, which is associated with a ~7% reduction in the volume of $(Fe,Si)O_6$ octahedra (**Table S1**).

The bulk moduli of $Ski_{76.6}Maj_{23.4}$ garnet with iron in the high-spin and low-spin states are remarkably different at the pressure of the spin crossover 50-60 GPa: $K_{300,\ 60\ (High\ Spin)}$= 381(2) GPa and $K_{300,\ 60\ (Low\ Spin)}$=531(19) GPa. The latter value was obtained from a fit using a 2nd order Birch-Murnaghan equation of state (K´ fixed at 4) of the P-V data at pressures above 60 GPa. The bulk moduli of $(Fe,Si)O_6$ octahedra with iron in the high-spin and low-spin states are significantly different as well: $K((Fe,Si)O_6)_{300,60}$ = 435(3) GPa and $K((Fe,Si)O_6)_{300,60}$=496(2) GPa, respectively (K´ fixed at 4).

4.3 Does the type of cation occupying the dodecahedral site define the compressibility of garnet?

Based on density functional theory, Milman et al. (2001) suggested that the bulk modulus of garnet is strongly affected by the bulk modulus of the dodecahedra, while the compressibilities of other individual polyhedra (tetrahedra and octahedra) do not correlate with the bulk compressibility of the material. Dymshits et al. (2014) claimed that, in this case, Na-majorite $Na_2MgSi_5O_{12}$ would have the smallest bulk modulus with Na in the dodecahedral position, while experimental observations show the opposite result: Na-majorite has the highest bulk modulus (184(4) GPa) with the lowest unit-cell volume (1475.9 $Å^3$), despite the large Na (1.07 Å) atom in the dodecahedral position. Friedrich et al. (2014, 2015) studied the Ca-bearing garnets andradite $Ca_3Fe_2Si_3O_{12}$ and henritetmenite $Ca_3Mn_2[SiO_4]_2[O_4H_4]$. While the overall bulk moduli of these garnets are significantly different (andradite- 161(4) GPa and

henritetmenite- 101(1) GPa), the bulk moduli of dodecahedra in these garnets (104 GPa for andradite and 101.2(4) GPa and 88.4(8) GPa for henritermierite) are much closer.

In the skiagite-Fe-majorite garnets studied in this work, dodecahedral sites are occupied exclusively by Fe^{2+} and the bulk moduli of dodecahedra are within the range 112-115 GPa. If the compressibility of dodecahedra was indeed the main factor that determined the bulk compressibility of garnet, all of the skiagite-Fe-majorite garnets that we investigated should have had the same bulk moduli. However, all four garnets with five different compositions (taking into account pure skiagite) have different bulk moduli **(Table S5**). Thus, our results support the idea of Dymshits et al. (2014) that the compression mechanism of garnet is complex, and suggests that not only the compressibility of individual polyhedra is relevant, but also the behavior of the polyhedral framework and the bending angle between the octahedra and tetrahedra.

Implication

The iron majorite endmember $Fe_4Si_4O_{12}$ is not stable, but the solid-solution $Fe_3Al_2Si_3O_{12}$–$Fe_4Si_4O_{12}$ has been shown to extend to at least 40 mol. % $FeSiO_3$ (Akaogi and Akimoto 1977). There have been several studies in the system $Mg_4Si_4O_{12}$–$Fe_4Si_4O_{12}$ majorite focusing on phase stability and crystal structures of garnets (Kato 1986; Matsubara et al. 1990; Ohtani et al. 1991; Tomioka et al. 2002; McCammon and Ross 2003). However, the effect of iron-majorite substitution on the compressibility of garnets is unknown.

Pyrope-majorite garnets have been studied using Brillouin spectroscopy (Sinogeikin and Bass 2002; Gwanmesia et al. 2009). Their results demonstrated that the zero-pressure bulk modulus of Py_{50}-Mj_{50} and $Py_{60}Mj_{40}$ decreases slightly (from 172(2) to 169(1) GPa, essentially within the uncertainty of measurements) with a decrease of the majorite component. Recent work by Dymshits et al. (2014) reports a small increase of the bulk modulus compare to pure knorringite garnet from 153.4(9) GPa to 157(2) GPa in knorringite-

majorite garnet ($Mg_{3.19}Cr_{1.60}Si_{3.19}O_{12}$) with admixture of 19% of a majorite component ($Mg_4Si_4O_{12}$). Hazen et al. (1994) conducted single-crystal X-ray diffraction studies of majorites with different compositions: Ca-bearing majorite ($(Ca_{0.49}Mg_{2.51})(Mg,Si)Si_3O_{12}$) (K=164.8(2.3) GPa), Na-bearing majorite ($(Na_{0.37}Mg_{2.48})(Mg_{0.13}Al_{1.07}Si_{0.80})Si_3O_{12}$) (K=175.1(1.3) GPa), and ($(Na_{1.88}Mg_{0.22})(Mg_{0.06}Si_{1.94})Si_3O_{12}$) (K=191.5(2.5) GPa. The isothermal bulk modulus of these garnets increases with increasing majorite component.

Figure 5 (a) shows the variation of the bulk moduli of different garnets as a function of majorite content. It is obvious that an increase of the majorite component causes an increase of the bulk modulus for Fe-bearing (this study, Woodland et al.1999), Cr-bearing (Dymshits et al. 2014), and Na and Ca-bearing (Hazen et al., 1994; Dymshits et al., 2014) majorites. In contrast, the pyrope-majorite ($Mg_3Al_2Si_3O_{12}$-$Mg_4Si_4O_{12}$) join shows a different behavior and a low (~160 GPa) value of the bulk modulus for pure Mg-majorite (Liu et al. 2000; Sinogeikin and Bass 2000). A similarly low value of 168 GPa is reported by Li and Liebermann, 2007) for Mg-majorite. We note that extrapolation of our data gives 178 GPa for pure Fe-majorite. Knowledge of the density ρ and the bulk modulus K allows a calculation of the bulk sound velocity $V_B = \sqrt{K/\rho}$ **(Table 5).** Extrapolation of our data for the pure Fe-majorite composition gives a value of 6.37 km/s, which is significantly lower than any estimates for the Mg-majorite end member **(Fig. 5b).**

Thus, our results for majorite firmly establish that the total iron content and the Fe^{2+}/Fe^{3+} ratio notably affect its elastic properties and the bulk sound velocity. Both therefore need to be included in the interpretation of seismological data to model the composition of the Earth's upper mantle and transition zone. While current data on the pressure and temperature dependence of the elasticity of Fe-bearing garnets are too limited for detailed quantitative analysis, our results provide a strong motivation for further studies in this area.

4 Conclusions

We studied skiagite-Fe-majorite garnet with four different compositions by means of synchrotron single-crystal X-ray diffraction and synchrotron Mössbauer source spectroscopy at pressures up to 90 GPa. The data on the compressibility of Fe-bearing garnets acquired in this work combined with analysis of literature data unambiguously demonstrate the influence of total iron content and Fe^{3+}/Fe^{2+} ratio in majorite on its elasticity. Thus, modelling of the composition of garnet-rich regions of the Earth's interior (the upper mantle and transition zone, in particular) and interpretation of seismological data should consider the effect of iron and its oxidation state.

We note the anomalous compressional behavior of Fe-bearing garnets along the skiagite-Fe-majorite join in the pressure range of 50 to 60 GPa. The compressibility of individual cation polyhedra combined with data from Mössbauer spectroscopy suggests spin crossover of both ferrous and ferric iron in $(Fe,Si)O_6$ octahedra in the garnet structure.

Acknowledgments

We acknowledge the ESRF and DESY for provision of synchrotron radiation facilities. This study was partly supported by the Russian Foundation for Basic Research (project no. 16-05-00419).

Reference

Ahrens, T.J. (1995) Mineral physics and Crystallography, a handbook of physical constants, 64-97 p. AGU Publications, Washington DC.

Akaogi, M., and Akimoto, S. (1977) Pyroxene-garnet solid-solution equilibria in the systems $Mg_4Si_4O_{12}$-$Mg_3Al_2Si_3O_{12}$ and $Fe_4Si_4O_{12}$-$Fe_3Al_2Si_3O_{12}$. Physics of the Earth and Planetary Interiors, 15, 90–106.

Amthauer, G., Annersten, H., and Hafner, S.S. (1976) The Mössbauer spectrum of ^{57}Fe in silicate garnets. Zeitschrift für Kristallographie- …, 143, 14–55.

Angel, R.J., Gonzalez-Platas, J., and Alvaro, M. (2014) EosFit7c and a Fortran module (library) for equation of state calculations. Zeitschrift fur Kristallographie, 229, 405–419.

Badro, J., Fiquet, G., Struzhkin, V. V, Somayazulu, M., Mao, H., Shen, G., and Le Bihan, T. (2002) Nature of the high-pressure transition in Fe_2O_3 hematite. Physical review letters, 89, 205504.

Bengtson, A., Li, J., and Morgan, D. (2009) Mossbauer modeling to interpret the spin state of iron in (Mg,Fe)SiO_3 perovskite. Geophysical Research Letters, 36, L15301/1–L15301/5.

Bobrov, A. V., Kojitani, H., Akaogi, M., and Litvin, Y.A. (2008) Phase relations on the diopside–jadeite–hedenbergite join up to 24GPa and stability of Na-bearing majoritic garnet. Geochimica et Cosmochimica Acta, 72, 2392–2408.

Bykova, E., Bykov, M., Prakapenka, V., Konôpková, Z., Liermann, H.-P., Dubrovinskaia, N., and Dubrovinsky, L.S. (2013a) Novel high pressure monoclinic Fe_2O_3 polymorph revealed by single-crystal synchrotron X-ray diffraction studies. High Pressure Research, 33, 534–545.

Bykova, E., Bobrov, A. V., Sirotkina, E. a., Bindi, L., Ovsyannikov, S. V., Dubrovinsky, L.S., and Litvin, Y. a. (2013b) X-ray single-crystal and Raman study of knorringite, $Mg_3(Cr_{1.58}Mg_{0.21}Si_{0.21})Si_3O_{12}$, synthesized at 16 GPa and 1,600 °C. Physics and Chemistry of Minerals, 41, 267–272.

Cerantola, V., McCammon, C., Kupenko, I., Kantor, I., Marini, C., Wilke, M., Ismailova, L., Solopova, N., Chumakov, A., Pascarelli, S., and others (2015) High-pressure spectroscopic study of siderite ($FeCO_3$) with a focus on spin crossover. American Mineralogist, 100, 2670–2681.

Duffy, T.S., and Anderson, D.L. (1989) Seismic velocities in mantle minerals and the mineralogy of the upper mantle. Journal of Geophysical Research, 94, 1895.

Dymshits, A.M., Litasov, K.D., Shatskiy, A., Sharygin, I.S., Ohtani, E., Suzuki, A., Pokhilenko, N.P., and Funakoshi, K. (2014) P – V – T equation of state of Na-majorite to 21 GPa and 1673 K. Physics of the Earth and Planetary Interiors, 227, 68–75.

Dymshits, A.M., Litasov, K.D., Sharygin, I.S., Shatskiy, A., Ohtani, E., Suzuki, A., and Funakoshi, K. (2014) Thermal equation of state of majoritic knorringite and its significance for continental upper mantle. Journal of Geophysical Research B: Solid Earth, 1–13.

Fei, Y., Ricolleau, A., Frank, M., Mibe, K., Shen, G., and Prakapenka, V. (2007) Toward an internally consistent pressure scale. Proceedings of the National Academy of Sciences of the United States of America, 104, 9182–9186.

Friedrich, A., Winkler, B., Morgenroth, W., Ruiz-Fuertes, J., Koch-Müller, M., Rhede, D., and Milman, V. (2014) Pressure-induced spin collapse of octahedrally coordinated Fe^{3+} in $Ca_3Fe_2[SiO_4]_3$. Physical Review B, 90, 094105.

Friedrich, A., Winkler, B., Morgenroth, W., Perlov, A., and Milman, V. (2015) Pressure-induced spin collapse of octahedrally coordinated Mn^{3+} in the tetragonal hydrogarnet henritermierite $Ca_3Mn_2[SiO_4]_2[O_4H_4]$. Physical Review B - Condensed Matter and Materials Physics, 92.

Gwanmesia, G.D., Wang, L., Triplett, R., and Liebermann, R.C. (2009) Pressure and temperature dependence of the elasticity of pyrope–majorite [$Py_{60}Mj_{40}$ and $Py_{50}Mj_{50}$] garnets solid solution measured by ultrasonic interferometry technique. Physics of the Earth and Planetary Interiors, 174, 105–112.

Hazen, R.M., Downs, R.T., Conrad, P.G., Finger, L.W., and Gasparik, T. (1994) Comparative compressibilities of majorite-type garnets. Physics and Chemistry of Minerals, 21, 1994.

Heinemann, S., Sharp, T.G., and Seifert, F. (1997) The cubic-tetragonal phase transition in the system majorite and garnet symmetry in the Earth's transition zone. Physics and Chemistry of Minerals, 24, 206–221.

Hsu, H., Blaha, P., Cococcioni, M., and Wentzcovitch, R.M. (2011) Spin-State Crossover and Hyperfine Interactions of Ferric Iron in $MgSiO_3$ Perovskite. Physical Review Letters, 106, 118501.

Irifune, T., Higo, Y., Inoue, T., Kono, Y., Ohfuji, H., and Funakoshi, K. (2008) Sound velocities of majorite garnet and the composition of the mantle transition region. Nature, 451, 814–817.

Ismailova, L., Bobrov, A., Bykov, M., Bykova, E., Cerantola, V., Kupenko, I., McCammon, C., Dyadkin, V., Chernyshov, D., Pascarelli, S., and others (2015) High-pressure synthesis of skiagite-majorite garnet and investigation of its crystal structure. American Mineralogist, 100, 2650–2654.

Ita, J., and Stixrude, L. (1992) Petrology, elasticity, and composition of the mantle transition. Journal of Geophysical Research, 97(B5), 6849–6866.

Kantor, I., Dubrovinsky, L., and McCammon, C. (2006) Spin crossover in (Mg,Fe)O: A Mössbauer effect study with an alternative interpretation of x-ray emission spectroscopy data. Physical Review B, 73, 100101.

Kato, T. (1986) Stability relation of $(Mg,Fe)SiO_3$ garnets, major constituents in the Earth's interior. Earth and Planetary Science Letters, 77, 399–408.

Lavina, B., Dera, P., Downs, R.T., Prakapenka, V., Rivers, M., Sutton, S., and Nicol, M. (2009) Siderite at lower mantle conditions and the effects of the pressure-induced spin-pairing transition. Geophysical Research Letters, 36, 1–4.

Li, B., and Liebermann, R.C. (2007) Indoor seismology by probing the Earth ' s interior by using sound velocity measurements at high pressures and temperatures. Proceedings of the National Academy of Sciences, 104(22), 9145–9150.

Liermann, H.-P., Konôpková, Z., Morgenroth, W., Glazyrin, K., Bednarčik, J., McBride, E.E., Petitgirard, S., Delitz, J.T., Wendt, M., Bican, Y., and others (2015) The Extreme Conditions Beamline P02.2 and the Extreme Conditions Science Infrastructure at PETRA III. Journal of Synchrotron Radiation, 22, 1–17.

Liu, J., Chen, G., Gwanmesia, G.D., and Liebermann, R.C. (2000) Elastic wave velocities of a pyrope-majorite garnets ($Py_{62}Mj_{38}$ and $Py_{50}Maj_{50}$ to 9 GPa. Physics of the Earth and Planetary Interiors, 120, 153–163.

Luth, R.W., Virgo, D., Boyd, F.R., Wood, B.J., Geoinstitut, B., Bayreuth, U., Bayreuth, D.-, and Republic, F. (1990) Ferric iron in mantle-derived garnets. Implications for thermobarometry and for the oxidation state of the mantle, 104, 56–72.

Matsubara, R., Toraya, H., Tanaka, S., and Sawamoto, H. (1990) Precision lattice-parameter determination of (Mg,Fe)SiO3 tetragonal garnets. Science, 697–699.

McCammon, C.A., and Ross, N.L. (2003) Crystal chemistry of ferric iron in (Mg,Fe)(Si,Al)O3 majorite with implications for the transition zone. Physics and Chemistry of Minerals, 30, 206–216.

Merlini, M., Hanfland, M., Gemmi, M., Huotari, S., Simonelli, L., and Strobel, P. (2010) Fe^{3+} spin transition in $CaFe_2O_4$ at high pressure. American Mineralogist, 95, 200–203.

Milman, V., Akhmatskaya, E. V., Nobes, R.H., Winkler, B., Pickard, C.J., and White, J.A. (2001) Systematic ab initio study of the compressibility of silicate garnets. Acta Crystallographica Section B: Structural Science, 57, 163–177.

Momma, K., and Izumi, F. (2011) VESTA 3 for three-dimensional visualization of crystal,

volumetric and morphology data. Journal of Applied Crystallography, 44, 1272–1276.

Novak, G.A., and Gibbs, G.V. (1971) The crystal chemistry of the silicate garnets. American Mineralogist, 56, 791–825.

Ohtani, E., Kagawa, N., and Fujino, K. (1991) Stability of majorite (Mg,Fe)SiO_3 at high pressures and 1800 ^{0}C. Earth and Planetary Science Letters, 102, 158–166.

Oxford Diffraction (2006) CrysAlisPro. Oxford Diffraction Ltd, Abingdon, Oxfordshire, England.

Petříček, V., Dušek, M., and Palatinus, L. (2014) Crystallographic Computing System JANA2006: General features. Zeitschrift für Kristallographie, 229, 345–352.

Prescher, C., McCammon, C., and Dubrovinsky, L. (2012) MossA : a program for analyzing energy-domain Mössbauer spectra from conventional and synchrotron sources. Journal of Applied Crystallography, 45, 329–331.

Ringwood, A.E. (1975) Composition and petrology of the Earth's upper mantle.

Rüffer, R., and Chumakov, A.I. (1996) Nuclear Resonance Beamline at ESRF. Hyperfine Interactions, 97-98, 589–604.

Sinogeikin, S. V., and Bass, J.D. (2000) Single-crystal elasticity of pyrope and MgO to 20 GPa by Brillouin scattering in the diamond cell. Physics of the Earth and Planetary Interiors, 120, 43–62.

Sinogeikin, S. V, and Bass, J.D. (2002) Elasticity of pyrope and majorite-pyrope solid solutions to high temperatures. Earth and Planetary Science Letters, 203, 549–555.

Sirotkina, E.A., Bobrov, A. V., Bindi, L., and Irifune, T. (2015) Phase relations and formation of chromium-rich phases in the system $Mg_4Si_4O_{12}$–$Mg_3Cr_2Si_3O_{12}$ at 10–24 GPa and 1,600 °C. Contributions to Mineralogy and Petrology, 169.

Stan, C. V, Wang, J., Zouboulis, I.S., Prakapenka, V., and Duffy, T.S. (2015) High-pressure phase transition in $Y_3Fe_5O_{12}$. Journal of Physics: Condensed Matter, 27, 405401.

Tomioka, N., Fujino, K., Ito, E., Katsura, T., Sharp, T.G., and Kato, T. (2002) Microstructures and structural phase transition in (Mg,Fe)SiO_3 majorite. European Journal of Mineralogy, 14, 7–14.

Wood, B.J., Pawley, A., and Frost, D. (1996) Water and carbon in the Earth's mantle. Philosophical Transactions of the Royal Society of London, 354, 1495–1511.

Wood, B.J., Kiseeva, E.S., and Matzen, a. K. (2013) Garnet in the Earth's Mantle. Elements, 9, 421–426.

Woodland, a. B., Bauer, M., Ballaran, T.B., and Hanrahan, M. (2009) Crystal chemistry of $Fe_3^{2+}Cr_2Si_3O_{12}$-$Fe_3^{2+}Fe_2^{3+}Si_3O_{12}$ garnet solid solutions and related spinels. American Mineralogist, 94, 359–366.

Woodland, A.B., and Koch, M. (2003) Variation in oxygen fugacity with depth in the upper mantle beneath the Kaapvaal craton , Southern Africa. Earth and Planetary Science Letters, 214, 295–310.

Woodland, A.B., and Ross, C.R. (1994) A crystallographic and Mössbauer spectroscopy study of Fe3Al2Si3O12–Fe32+Fe23+Si3O12 and Ca3Fe32+Si3O12. Physic and Chemistry of Minerals, 21, 117–132.

Woodland, A.B., Angel, R.J., Koch, M., Kunz, M., and Miletich, R. (1999) Equations of state

for $Fe_3Fe_2Si_3O_{12}$ and Fe_2SiO_4-Fe_3O_4 spinel solid solutions. Journal of Geophysical Research, 104, 20049–20058.

Xu, W., Greenberg, E., Rozenberg, G.K., Pasternak, M.P., Bykova, E., Boffa-Ballaran, T., Dubrovinsky, L., Prakapenka, V., Hanfland, M., Vekilova, O.Y., and others (2013) Pressure-induced hydrogen bond symmetrization in iron oxyhydroxide. Physical Review Letters, 111, 1–5.

List of figure captions

Table 1: Results of the crystal structure refinement based on single-crystal X-ray diffraction data for skiagite-majorite garnets with four different compositions.

Table 2: Bond lengths and volumes of octahedra in skiagite-majorite garnets at ambient conditions

Table 3: Equation of state coefficients obtained with a 3rd Birch-Murnaghan and Vinet EOS.

Table 4: Hyperfine parameter at selected pressures for skiagite-majorite garnet with composition ($Fe^{2+}_3(Fe^{2+}_{0.234(2)}Fe^{3+}_{1.532(1)}Si^{4+}_{0.234(2))}Si_3O_{12}$).

Table 5: Compositions, densities and bulk sound velocities of garnets at ambient conditions with different majorite contents.

Figure 1: Unit cell volume across the skiagite-majorite join showing linear behavior as a function of composition. Filled circles- this study, open circle - (Woodland and Ross 1994), open square – pure iron majorite as obtained by extrapolation of solid solution data along the almandine-majorite join (Akaogi and Akimoto 1977). Errors are less than the symbol size.

Figure 2: Compressibility of skiagite-majorite garnet with four different compositions (a – $Fe^{2+}_3(Fe^{2+}_{0.234(2)}Fe^{3+}_{1.532(1)}Si^{4+}_{0.234(2)})Si_3O_{12}$; b – $Fe^{2+}_3(Fe^{2+}_{0.31(2)}Fe^{3+}_{1.39(2)}Si^{4+}_{0.31(2)})Si_3O_{12}$; c – $Fe^{2+}_3(Fe^{2+}_{0.46(2)}Fe^{3+}_{1.08(2)}Si^{4+}_{0.46(2)})Si_3O_{12}$; d – $Fe^{2+}_3(Fe^{2+}_{0.76(5)}Fe^{3+}_{0.48(5)}Si^{4+}_{0.76(5)})Si_3O_{12}$. The error bars are comparable to the symbol size. The results of fits using a 3rd order Birch-Murnaghan equation of state are shown by solid lines.

Figure 3: (a) Normalized polyhedral volume compression of skiagite-majorite garnet $Ski_{76.6}Maj_{23.4}$ (b) Polyhedral volume compression of skiagite-majorite garnet $Ski_{76.6}Maj_{23.4}$. Solid lines represent the fit of the P-V data using a 2nd order Birch-Murnaghan equation of state (K´=4).

Errors are smaller than the symbol size. The gray bar indicates the pressure region of the iron high-spin to low-spin transition.

Figure 4: Selected Mössbauer spectra of skiagite-majorite garnet ($Fe^{2+}_3(Fe^{2+}_{0.234(2)}Fe^{3+}_{1.532(1)}Si^{4+}_{0.234(2)})Si_3O_{12}$) at (*a*) ambient, at (*b*) 49.6(5) GPa , at 56.0(5) GPa. Hyperfine parameters are shown in Table 4. Green doublet – high-spin Fe^{2+} in

dodecahedra, blue doublet – high-spin Fe^{3+} in octahedra, red doublet – low-spin Fe^{3+} in octahedra, turquoise singlet – low-spin Fe^{2+} in octahedra)

Figure 5: Variation of (a) isothermal bulk moduli and (b) bulk sound velocities of garnets at 300 K as a function of majorite content as revealed by the present study and literature data. Red circles – skiagite-majorite garnets (this study) and pure skiagite (Woodland et al. 1999); red squares – Ca-bearing and Na-bearing majorite (Hazen et al. 1994); red triangle– majoritic knorringite (Dymshits et al., 2014); inverted red triangle– Na-majorite (Dymshits et al., 2014), blue triangle– "pyrolite minus olivine" majorite garnet $Py_{23}Alm_6Mj_{50}Gr_{21}$ (Irifune et al. 2008); blue circle – Mg-majorite $Mg_4Si_4O_{12}$ (Li and Liebermann 2007); black circles – Mg-majorite garnets (Liu et al. 2000, Sinogeikin and Bass, 2000). Red lines represent linear fits of our experimental data. Error bars show the experimental uncertainties. When the value of bulk modulus was obtained with the Brillouin technique (K_s), it was converted to K_0 by applying the relationship $K_S=K_T(1+\alpha\gamma T)$, where α is thermal expansion, γ is the Grüneisen parameter, and T is temperature. The values of α and γ for skiagite-majorite garnets were assumed to be equal to those of pyrope and were taken from (Ahrens 1995).

523 **Table 1**

524

Run number and composition	**S6073** **$Ski_{76.6}Maj_{23.4}$**	**S6176** **$Ski_{69}Maj_{31}$**	**S6177** **$Ski_{54}Maj_{46}$**	**S6160** **$Ski_{24}Maj_{76}$**
P, T conditions of synthesis	9.5 GPa 1400 K	9.5 GPa 1600 K	9.5 GPa 1500 K	7.5 GPa 1400 K
Crystal system Space group	cubic $Ia\bar{3}d$			
Z	8			
λ(Å)	0.41505			
a (Å)	11.7210(2)	11.71620(10)	11.7053(4)	11.68130(10)
V ($Å^3$)	1610.25(5)	1608.28(2)	1603.79(9)	1593.95(2)
F(000)	2117	2114	2100	2068
Theta range for data collection (°)	2.658/17.585	1.742/17.821	1.748/17.795	2.49/22.03
Index ranges	-15 < h < 12,	-15 < h < 17,	-17< h < 14,	-20 < h < 21,
	-18 < k < 17,	-20< k < 19,	-15< k < 13,	-16 < k < 13,
	-17< l <13	-15< l <13	-20< l <19	-15< l <16
No. of measured, independent, and observed [I > 3s(I)] reflections	1626/269/ 219	1765/ 281/ 221	1655/ 267/181	1955/ 296/182
R_{int}	0.0337	0.0316	0.0752	0.0415
No.of parameters/restraints/ constraints	18/0/2	18/0/2	18/0/2	18/0/2
Final R indices [I > 3σ(I)] R_F / wR_F	0.0326/0.0417	0.0300/ 0.0470	0.0653/0.0821	0.0868/ 0.1020
R indices (all data) R_F / wR_F	0.0394/0.0443	0.0381/0.0497	0.0781/ 0.0852	0.1491/ 0.1630

525

526

527

528

529

530 **Table 2**

Composition	**Ski_{100}***	**$Ski_{76.6}Maj_{23.4}$**	**$Ski_{69}Maj_{31}$**	**$Ski_{54}Maj_{46}$**	**$Ski_{24}Maj_{76}$**
(Fe,Si)-O, Å	1.98	1.9818(13)	1.969(4)	1.9771(15)	1.957(5)
$(Fe,Si)O_6$, Å^3	10.40	10.3646	10.2914	10.1732	9.9780

531 *predicted by Novak and Gibbs (1971)

532 **Table 3**

	Birch-Murnaghan			Vinet			
Composition	$V_{0,}$ Å^3	$K_{0,300,}$ GPa	K'	$V_{0,}$ Å^3	$K_{0,300,}$ GPa	K'	References
Ski_{100}	1611.8(3)	157.4(3.0)	5.7(1.2)				(Woodland et al. 1999)
$Ski_{76.6}Maj_{23.4}$	1605.3(7)	159(1)	4.27(7)	1604.8(7)	160(1)	4.36(8)	this study
$Ski_{69}Maj_{31}$	1609(1)	168(1)	4.21(2)	1608(1)	168(1)	4.32(2)	this study
$Ski_{54}Maj_{46}$	1602(2)	170(2)	4.16(1)	1602(2)	170(2)	4.24(1)	this study
$Ski_{24}Maj_{76}$	1592.2(7)	172(1)	4.20(7)	1592.2(7)	172(1)	4.30(8)	this study

This is a preprint, the final version is subject to change, of the American Mineralogist (MSA)
Cite as Authors (Year) Title. American Mineralogist, in press.
(DOI will not work until issue is live.) DOI: http://dx.doi.org/10.2138/am-2017-5856

533 **Table 4**

534

Oxidation state	Position	Center shift (CS)* [mm/s]	Quadrupole splitting (QS) [mm/s]	Relative area [%]
Ambient				
Fe^{2+}	Dodecahedral	1.31(1)	3.45(2)	58(2)
Fe^{3+}	Octahedral	0.37(1)	0.26(2)	42(2)
49.6(5) GPa				
Fe^{2+}	Dodecahedral	1.17(1)	3.42(2)	58(3)
Fe^{3+}	Octahedral	0.23(2)	0.33(3)	42(3)
56.0(5) GPa				
Fe^{2+}	Dodecahedral	1.15(1)	3.41(3)	54(8)
Fe^{3+}	Octahedral	0.17(2)	0.4(2)	34(9)
Fe^{2+}	Octahedral	0.5	-	12(9)

535 Table 5

536

537

538

Composition	Density (calculated), g/cm^3	Bulk sound velocity, V_B (km/s)	References
Ski_{100}	4.58	5.86	(Woodland et al. 1999)
$Ski_{76.6}Maj_{23.4}$	4.49	5.93	this study
$Ski_{69}Maj_{31}$	4.51	6.10	this study
$Ski_{54}Maj_{46}$	4.49	6.15	this study
$Ski_{24}Maj_{76}$	4.45	6.22	this study
Mg Majorite $Mg_4Si_4O_{12}$	3.52	6.74	(Li and Liebermann 2007)
"Pyrolite minus olivine" $Py_{23}Alm_6Mj_{50}Gr_{21}$	3.605	6.70	(Irifune et al. 2008)

539

540

541

This is a preprint, the final version is subject to change, of the American Mineralogist (MSA)
Cite as Authors (Year) Title. American Mineralogist, in press.
(DOI will not work until issue is live.) DOI: http://dx.doi.org/10.2138/am-2017-5856

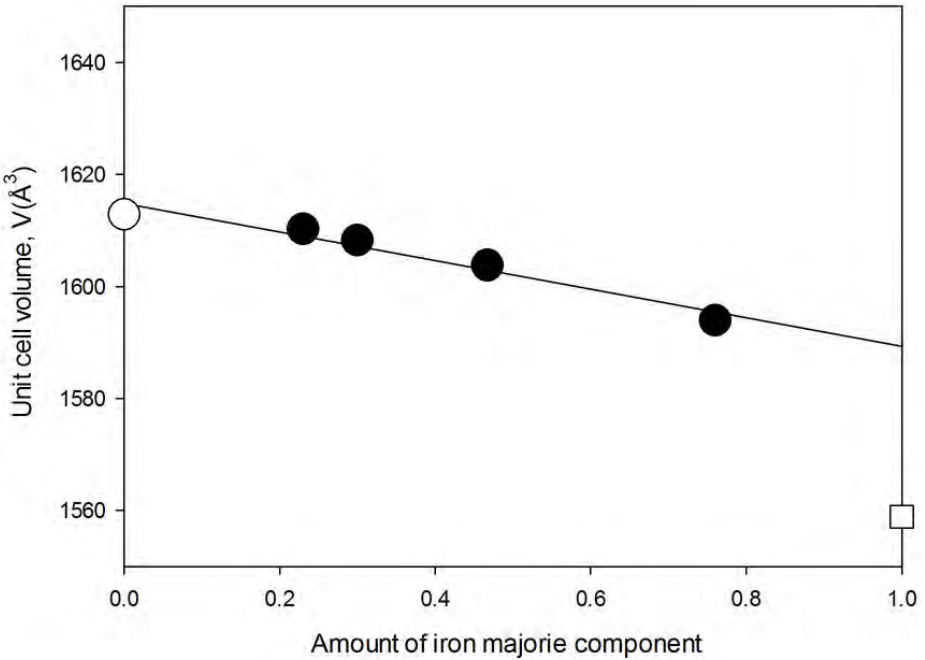

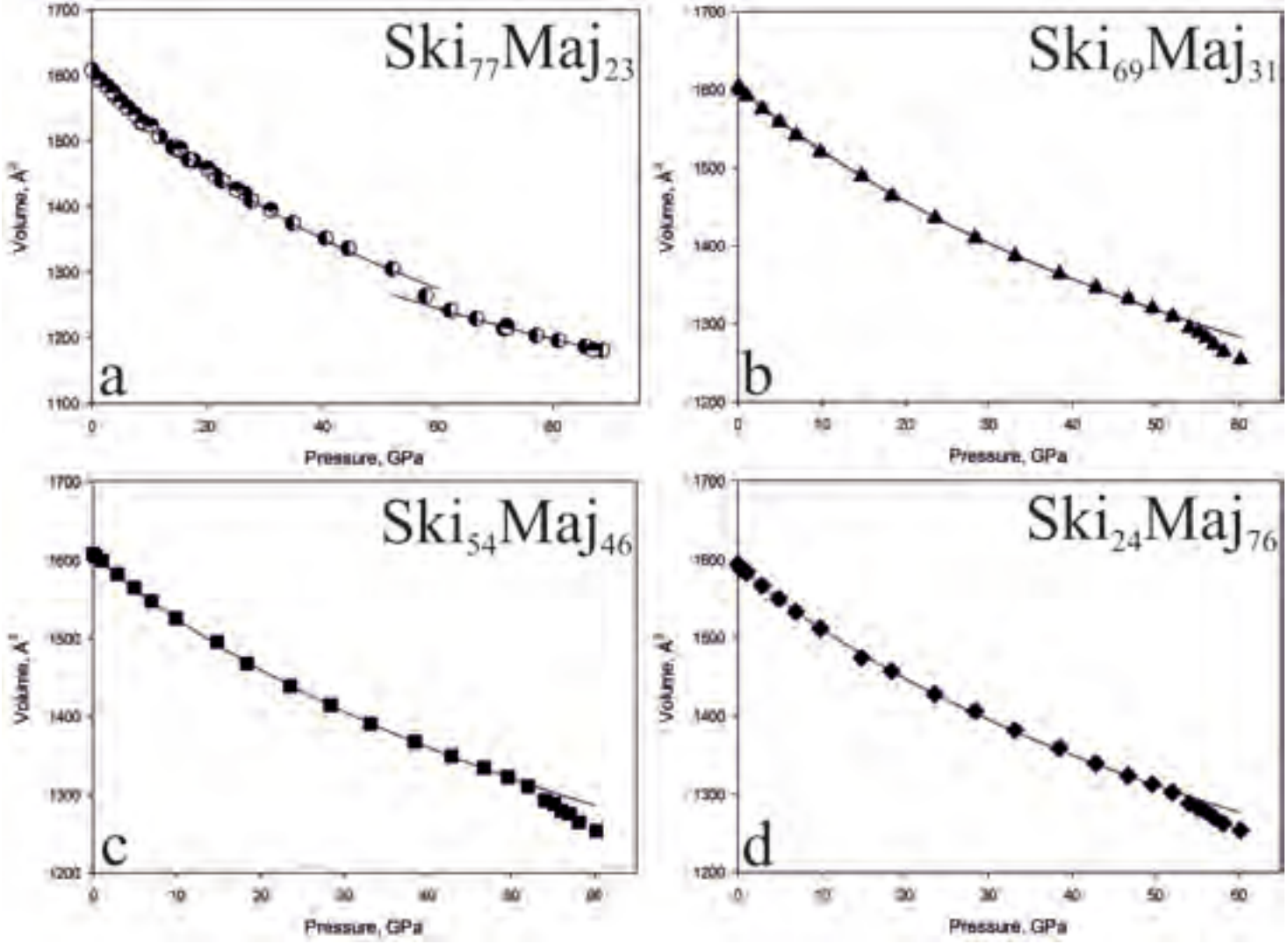

This is a preprint, the final version is subject to change, of the American Mineralogist (MSA)
Cite as Authors (Year) Title. American Mineralogist, in press.
(DOI will not work until issue is live.) DOI: http://dx.doi.org/10.2138/am-2017-5856

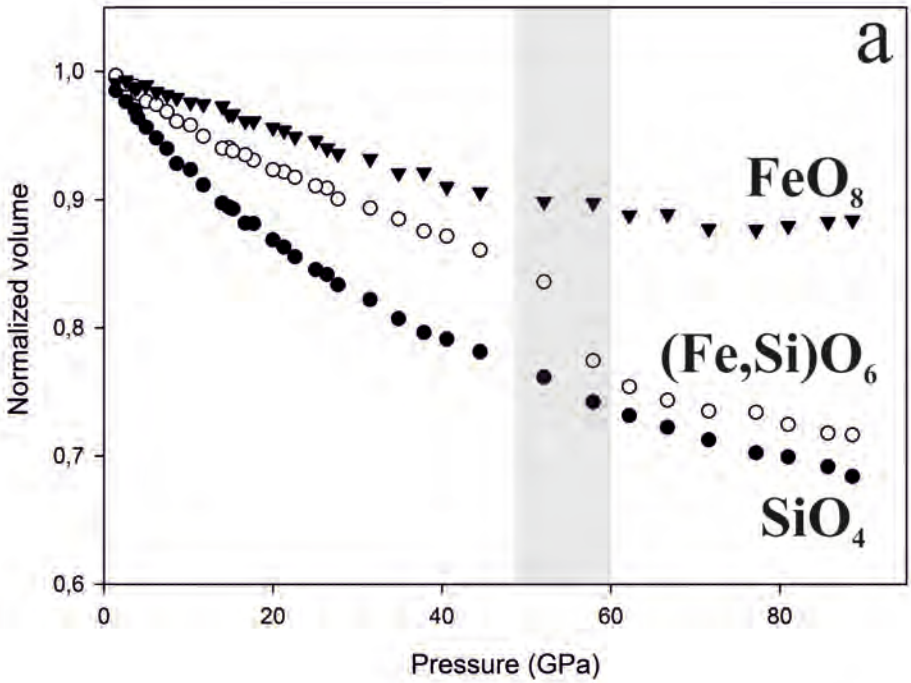

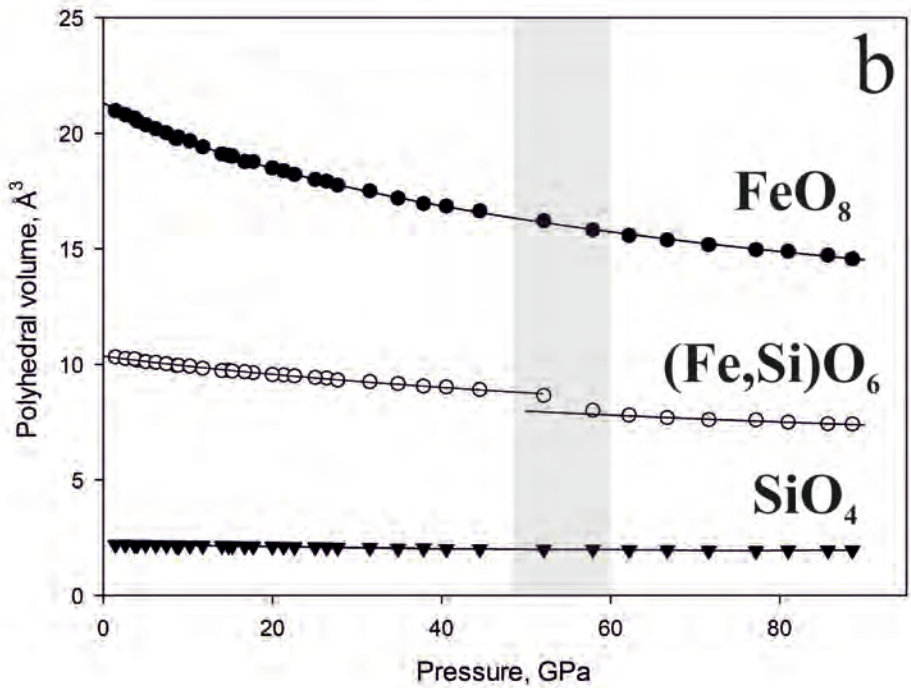

This is a preprint, the final version is subject to change, of the American Mineralogist (MSA)
Cite as Authors (Year) Title. American Mineralogist, in press.
(DOI will not work until issue is live.) DOI: http://dx.doi.org/10.2138/am-2017-5856

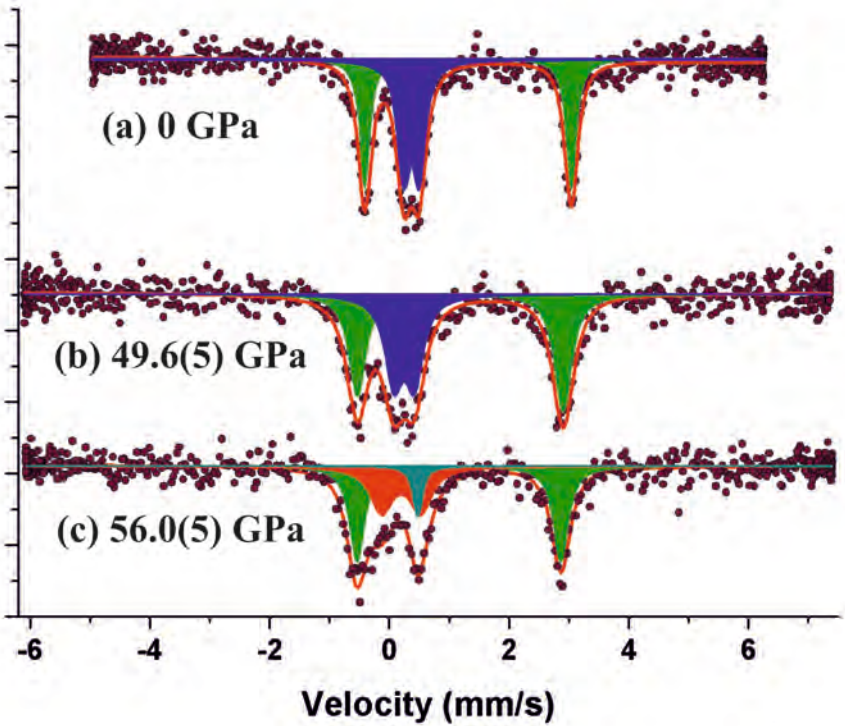

This is a preprint, the final version is subject to change, of the American Mineralogist (MSA)
Cite as Authors (Year) Title. American Mineralogist, in press.
(DOI will not work until issue is live.) DOI: http://dx.doi.org/10.2138/am-2017-5856